Journal of Applied Geophysics 67 (2009) 80–87

Contents lists available at ScienceDirect

Journal of Applied Geophysics

journal homepage: www.elsevier.com/locate/jappgeo

GPR prospecting in a prehispanic village, NW Argentina

Néstor Bonomo [a,b,*], Lorena Cedrina [a,b], Ana Osella [a,b], Norma Ratto [c]

[a] Departamento de Física, Facultad de Ciencias Exactas y Naturales, Universidad de Buenos Aires, Ciudad Universitaria, Pabellón 1, (1428) Buenos Aires, Argentina
[b] CONICET, Consejo Nacional de Investigaciones Científicas y Técnicas, Argentina
[c] Departamento de Arqueología, Facultad de Filosofía y Letras, Universidad de Buenos Aires, Argentina

ARTICLE INFO

Article history:
Received 31 May 2007
Accepted 25 September 2008

Keywords:
Geophysical prospecting
GPR
Archaeology

ABSTRACT

Palo Blanco is an approximately 1600 year old archaeological site located in Fiambalá Valley, in the Andean region of Argentina. Pioneer archaeological studies published in the 70s reported the existence of five residential units in this site. Also a small cemetery which included three circular tombs was discovered near to these buildings. Since that time, a profuse sedimentation covered the zone, so nowadays there are no evidences of most of these buildings on surface. Because of an imprecise location of the structures, most of the buildings became in fact missed. Then, in this work we aimed to re-localize two of the missed buildings, a residential unit and a tomb, by applying ground penetrating radar (GPR) methodology. We used fast fixed offset GPR configurations to investigate two areas in which these buildings could be expected. We used experimental and synthetic patterns to aid the identification of the characteristic signals due to the archaeological targets. We applied migration to the data to better define and resolve unclear anomalous signals. The employed methodology revealed the location of both buildings. Also a number of new non-reported structures were predicted and confirmed.

1. Introduction

The geophysical methods are increasingly applied to situations in which it is necessary to perform non-destructive shallow investigations, particularly in archaeological prospecting (Linford, 2006). Among these methods, the ground penetrating radar (GPR) is one of the most economical and best resolving techniques (Conyers and Goodman, 1997).

GPR surveys are often carried out by maintaining a fixed distance between the emitting and the receiving antennas (fixed offset or single folding surveys). This kind of deployment enables a quick prospecting, usually leading to a successful detection of a variety of archaeological targets, including walls, burials, cavities and other smaller objects such as pottery (Basile et al., 2000; Da Silva Cezar et al., 2001; Leopold and Völkel, 2004). On the other hand, variable offset surveys are often performed when it is necessary to increase the signal to noise ratio (Yilmaz, 1987). Although variable offset surveys can produce improved images of subsoil (Berard and Maillol, 2007), the acquisition and processing of the GPR data in this mode is much more time consuming.

Central frequencies around 500 MHz are often used in GPR applications to archaeology since they normally provide an adequate balance between resolution and penetration for a variety of targets and most of the soils (Conyers and Goodman, 1997). Higher frequencies, up to approximately 1 GHz, can be selected to obtain further details in the buried structures or to detect and characterize smaller objects. On the contrary, 50 MHz or 100 MHz antennas are commonly used to achieve greater penetrations, especially in cases with highly absorbent soils. Processing of the GPR data usually includes filtering, migration (Fisher et al., 1992; Jaya et al., 1999; Symes, 2007) and diverse visualization 2D, 2.5D and 3D techniques (Sigurdsson and Overgaard, 1998; Nuzzo et al., 2002; McClymont et al., 2008) that help in the interpretation of the subsoil characteristics.

Although the geophysical methods have been applied systematically in archaeology during the last decades, their implementation in Argentina is relatively new, having started at the end of the 1990s (e.g., Lascano et al., 2003; De la Vega et al., 2005; Osella et al., 2005). In 2004 we have began an archaeo–geophysical study in Palo Blanco site, NW Argentina. In the first stage of this study, we obtained a detailed map of one of the buried structures in this site, by applying the GPR and the dipole–dipole methods (Martino et al., 2006). This map made possible an efficient excavation of the structure. Continuing with this project, our next objective was to re-locate two missed buildings: a residential unit with adobe walls and a burial made from rocks. As we had to prospect relatively large areas in a short fieldwork, we decided to apply a fast fixed offset GPR methodology. To interpret the acquired data, both forward modeling and migration techniques were applied. This procedure allowed us to successfully establish the locations of the targets, which were afterwards confirmed by excavations.

2. The site

Palo Blanco archaeological site is centered at 67°44′46″W, 27°20′17″S, in Fiambalá Valley, a semi-desert region in Catamarca Province,

* Corresponding author. Departamento de Física, Facultad de Ciencias Exactas y Naturales, Universidad de Buenos Aires, Ciudad Universitaria, Pabellón 1, (1428) Buenos Aires, Argentina. Tel.: +54 11 4576 3353; fax: +54 11 4576 3357.
E-mail address: bonomo@df.uba.ar (N. Bonomo).

0926-9851/$ – see front matter © 2008 Elsevier B.V. All rights reserved.
doi:10.1016/j.jappgeo.2008.09.013

Argentina (Fig. 1a). This site is related to one of the first agricultural/pastoral communities of the region, which mainly developed during the Formative Period, approximately 1500–1700 years ago. The zone was abandoned by their original inhabitants, and probably remained uninhabited until the beginnings of the 20th century, when a small number of colonists settled some kilometres apart from the archaeological site.

Due to the geographic characteristics of the valley, the Palo Blanco zone is continuously exposed to an intense sedimentation. As a consequence, sediments in a short time usually bury objects that lay on the surface. The natural covering protects them against damaging agents, such as wind, summer flows, periodic changes in environmental humidity and radiation, and also cultural interaction. Although this process often made that the archaeological objects become imperceptible, parts of the buried objects can be occasionally exposed due to the natural movement of loose sediments through wind and water flows, making their detection possible.

In the 70's Sempé (1976, 1977) carried out the first archaeological studies in the zone. Sempé first studied a number of areas in which small portions of adobe walls had appeared on the surface. Five residential units with different architectural complexities were identified. According to Sempé's descriptions, these structures presented different shapes and spatial distributions though they all consisted of three or four rectangular shaped rooms directly connected or connected outdoors through partially open areas or courtyards. The residential units, which Sempé named NH1, NH2, NH3, NH4 and NH5, covered individual areas from 50 m^2 to 300 m^2 and were dispersed in a total area of approximately 9 ha (Fig. 1b). At present, sediments again covered practically all the architectural elements that were observed by the archaeologist. This resulted in a very low visibility of some of the structures or directly in no visibility of most of them.

The previous work by Sempé provided a preliminary description of the residential units; nevertheless more accurate descriptions are required in order to perform better evaluations about the architectural complexity of the site. It is necessary to note that the locations of the residential units and the layouts of the walls are not very clear in Sempé's reports. Then, it is a meaningful task to re-localize and to complete maps of the non-visible structures, in order to continue the archaeological research and to design preservation actions. In relation to this, the construction of a complete map of the residential units of Palo Blanco was proposed to adequately assess their social aspects and then to contribute to the analysis of the Formative Period (Ratto, 2005; Ratto et al., 2005).

In a previous work (Martino et al., 2006), a monostatic survey was carried out in the NH3 sector of Palo Blanco and a detailed map of the subsurface was obtained. These investigations confirmed Sempé's descriptions of this residential unit, and also a number of non-reported internal walls were predicted. The map of the buried structures was used to design an excavation plan, which allowed a subsequent time-efficient exposure of the whole unit and the confirmation of the geophysical predictions. We could check that portions of the adobe walls had collapsed and mixed up with the natural soil, and that a mudflow had deteriorated the northern part of the building. Though the materials of the walls did not differ from those in their surroundings, the applied GPR methodology produced clear electromagnetic signals from the walls and good resolutions. These results encouraged us to apply this kind of methodology to investigate wider areas in which similar or more deteriorated adobe structures could appear.

In the present stage of the multidisciplinary research in Palo Blanco, our first objective was to re-locate a missed residential unit, NH1, by applying a fast single fold GPR methodology. We prospected a zone located towards the S direction of the previously investigated NH3, which we named Sector 1 (Fig. 1b). The sector presented areas with small natural drainages and a number of slight depressions that were considered to be consequences of plundering of archaeological objects commonly known as *huaqueos* in the Andean region.

The second objective of this work was to study Sector 2, which was located approximately 800 m to the W of the NH buildings (Fig. 1b). This sector is interesting because local inhabitants found three funeral cists in this zone in the 50s. It was known that they had approximately semi-spherical forms and were constructed with rocks. The burials were opened in that occasion, although after some years they were covered again and the area was used as a vineyard for almost thirty years. Recently, within the scope of archaeological investigations, two

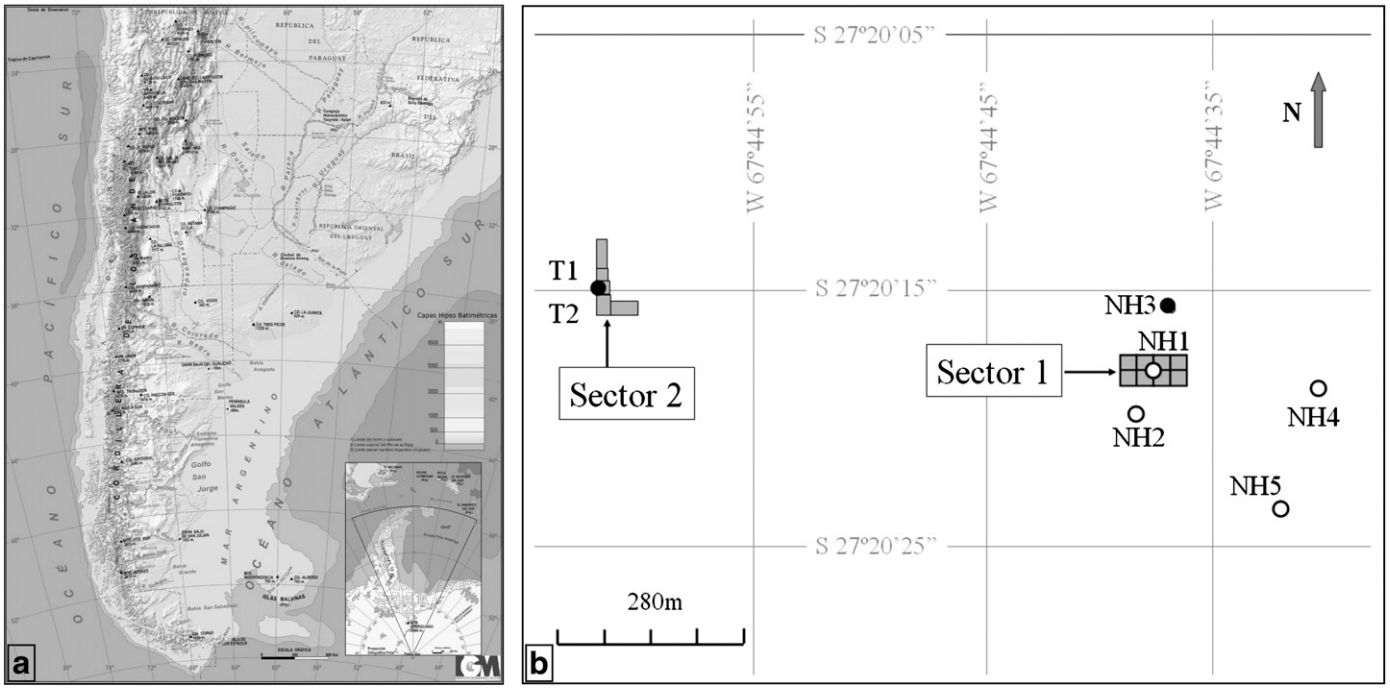

Fig. 1. a) Location of Palo Blanco archaeological site, Catamarca, Argentina, b) Map of the main archaeological structures in Palo Blanco. Solid circles mark formerly proved locations, and open circles mark possible locations. The prospected areas, Sector 1 and Sector 2, appear in grey.

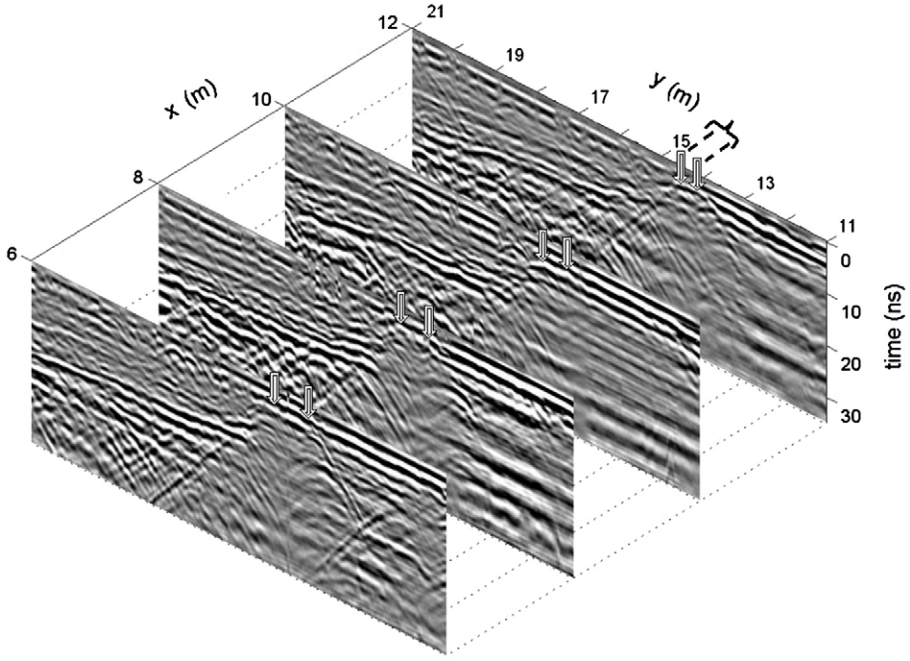

Fig. 2. A series of four radargrams performed in Sector 1. Characteristic anomalies can be observed in the radargrams around $y \approx 14.5$ m.

of these tombs, which we identified as T1 and T2, were located and excavated by the archaeologists (Ratto et al., 2007). They had mean diameters between 2.7 and 3.3 m, their walls extended from 0–20 cm to a maximum depth 1.2 m, and their widths were in the range 50–70 cm. Nevertheless the third tomb, T3, could not be found. Then, our second objective was to re-localize T3 by applying the mentioned GPR methodology. We estimated that the past agricultural activities in this zone probably destroyed the natural array of the shallowest strata and mixed up their materials, so weakly coherent electromagnetic signals could be expected for the archaeological targets below them. Furthermore, an appreciable amount of dispersed rocks were observed on surface, whose sizes were not negligible in relation to those of the rocks in the tombs. If there are also dispersed rocks embedded in the soil, they could produce secondary signals that hide the signals we searched for. Then, the analysis of the data from Sector 2 could result more complex than normal.

3. Prospecting of Sector 1

We centered Sector 1 at the possible location of NH1, as we interpreted from Sempé's reports. This consisted in a rectangular area, with lengths 100 m in the WE direction (x-axis) and 46 m in the NS direction (y-axis) (see Fig. 1b). We divided this area into smaller ones, with extensions 25 m × 25 m and 25 m × 24 m. This reduced the error in the longitudinal positions, mainly originated in occasional bad rotations of the odometer wheel in the loose sediments, as well as the error in the transverse direction.

Monostatic GPR profiles were performed using a system manufactured by Ingegneria Dei Sistemi (IDS) with a central frequency 400 MHZ. Cross line spacing was 1 m both in the WE and NS directions. We selected these values considering the expected dimensions and depths of the walls we searched for (mean heights 0.6 m, widths 0.6 m and maximum depths to the basis 1.5 m), the total area of the surveys (approximately 1 ha, including Sector 2) and the time we had to carry out them (two days). Forty traces per meter were acquired, which assured a good in-line resolution. Each trace had 256 data and a total duration of 60 ns.

We proccessed the data first by removing the direct signal, which hid a significant part of the range that could include the events of interest (up to 0.5 m, approximately). Then, a smooth bandpass filter was applied in the [0.2, 1.0] GHz range, thus eliminating those components outside the useful band. We applied gain to visualize the deeper signals; in this sector the gain factors were obtained from a smooth curve fitting performed on the values of the RMS average

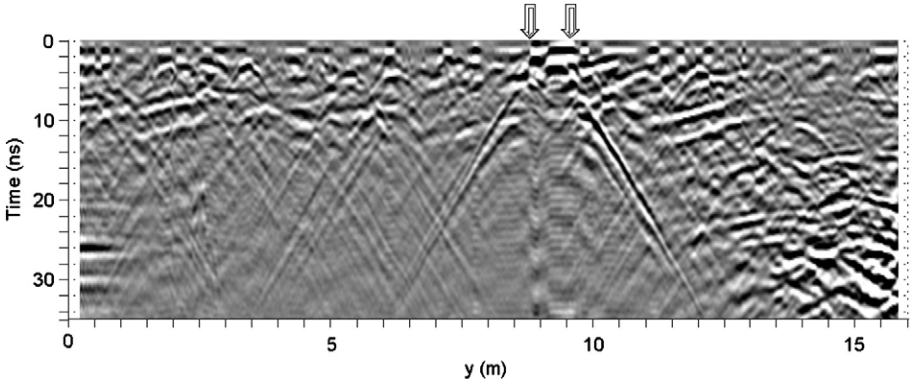

Fig. 3. Characteristic signals of a buried adobe wall. This radargram was obtained during the investigation of the neighbouring residential unit NH3 (from Martino et al., 2006).

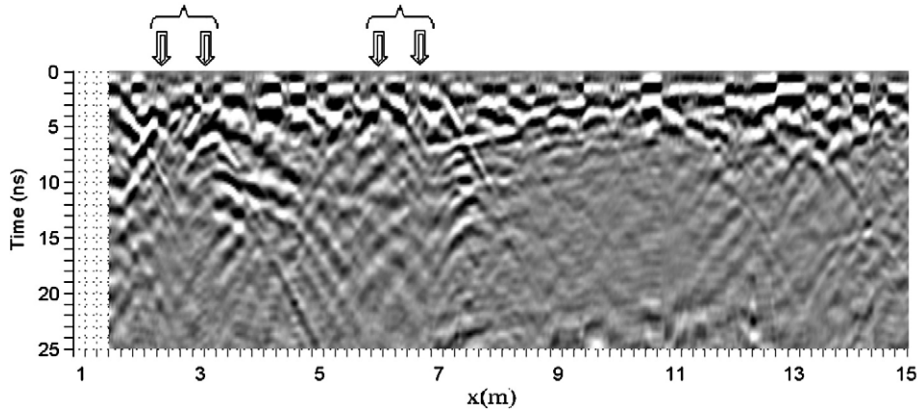

Fig. 4. Radargram obtained along $y=14$ m. Two (blurred) characteristic anomalies, which tops approximately extend from $x=2.4$ m to $x=3.2$ m, and from $x=6.0$ m to $x=7.0$ m, respectively, can be seen.

trace. Occasionally, a bandpass filter was applied along the direction of the radar scan in order to enhance weak diffraction signals that could be produced by archaeological targets, with respect to signals produced by horizontal or quasi-horizontal reflectors. In all the cases we used our own software to process the data, which was developed on Matlab platform.

In Fig. 2 we show a set of four radargrams acquired along the lines $x=6$ m, 8 m, 10 m and 12 m. In each of these radargrams, two opposite semi-hyperbolae, with vertices located approximately at $y=14$ m and $y=15$ m, respectively, can be observed. These signals are very similar to the characteristic ones produced by diffraction at the tops of the excavated walls in NH3 (the previously investigated sector); for example, Fig. 3 shows this kind of electromagnetic response (from Martino et al., 2006). The similarities between the detected anomalies and the previously obtained patterns and the repetitive appearance in successive profiles allow us to assume here the presence of a buried wall centered at 14.5 m and directed along the WE direction. It can be noted in Fig. 2 that other signs of the presence of vertical structures (walls) are the sudden interruption of the quasi-horizontal reflectors at about 15–20 ns and the lateral variation in the global signal pattern, especially for profiles at $x=6$ m and $x=8$ m.

If a wall was deteriorated by erosion or by a partial collapse and if sediments of similar properties were deposited close to it, their signals could become weaker or very different from the expected. Weak signals occur, for example, for the right branches of the characteristic signals in the radargrams along $x=8$ m and $x=12$ m, and also in $x=10$ m, although in the last profile the branch almost disappeared. Orthogonal radargram along $y=14$ m (Fig. 4) also presents two blurred characteristic anomalies, whose tops approximately extend from $x=2.4$ m to $x=3.2$ m, and from $x=6.0$ to $x=7.0$ m, respectively. As we

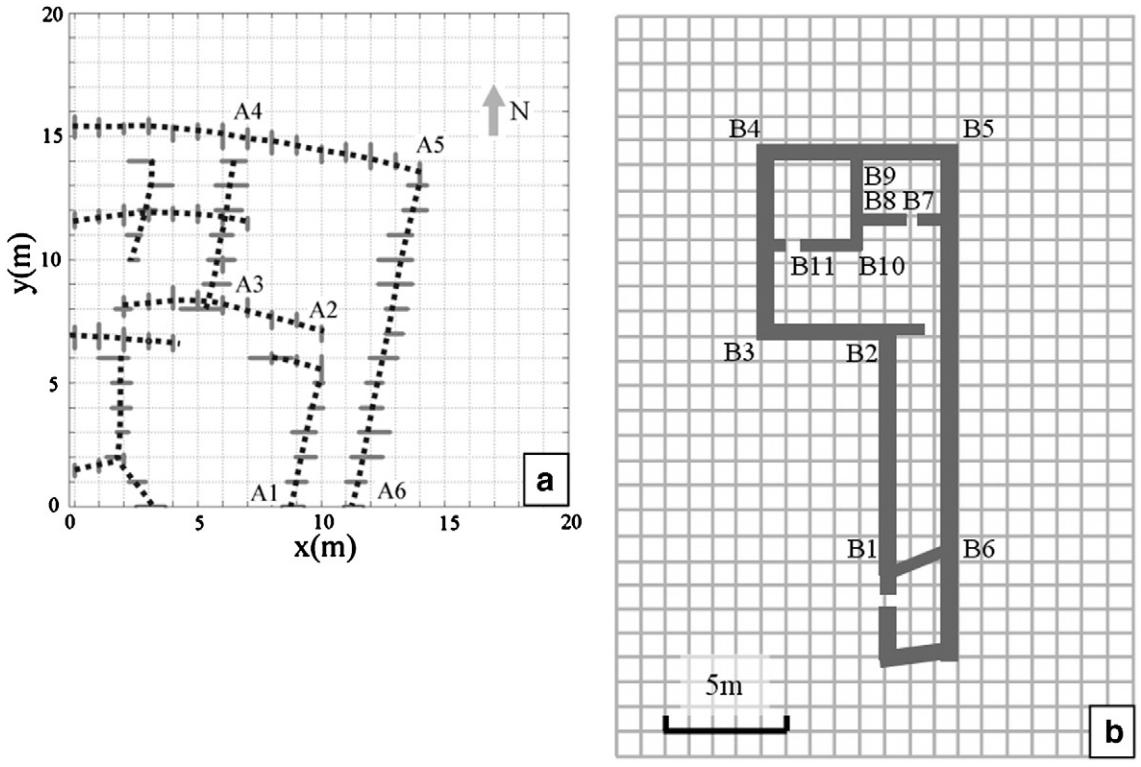

Fig. 5. a) Map of the main anomalies detected in Sector 1. The dashed lines indicate the possible layout of the walls of NH1. b) NH1, as we interpreted from Sempé's reports. The compared areas are indicated through letters in both figures.

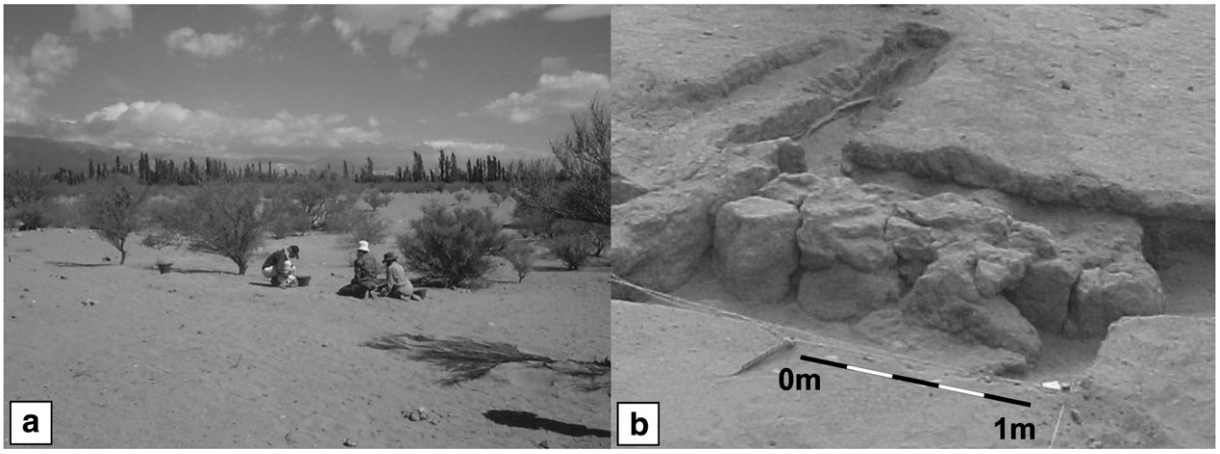

Fig. 6. a) A photograph of Sector 1. b) A partial excavation in one of the walls in Sector 1.

mentioned in the Introduction, further deterioration of the walls in Sector 1 was expected due to the summer flows, whose drainages could be observed on surface, besides wind action.

Following the methodology described in the above paragraphs, we identified all the anomalies in the sector. The widths of the anomalies were measured, which led to a range between 40 cm and 120 cm. In relation to this, we should note that the maximum width of the walls could be smaller than the mentioned for these anomalies, since possible mudflows could produce effective blocks wider than the actual walls. We also determined an approximate range of depths for the tops of the walls, which resulted 10–35 cm. To do this, we used an average velocity (19 cm/ns) which was estimated from the tails of the

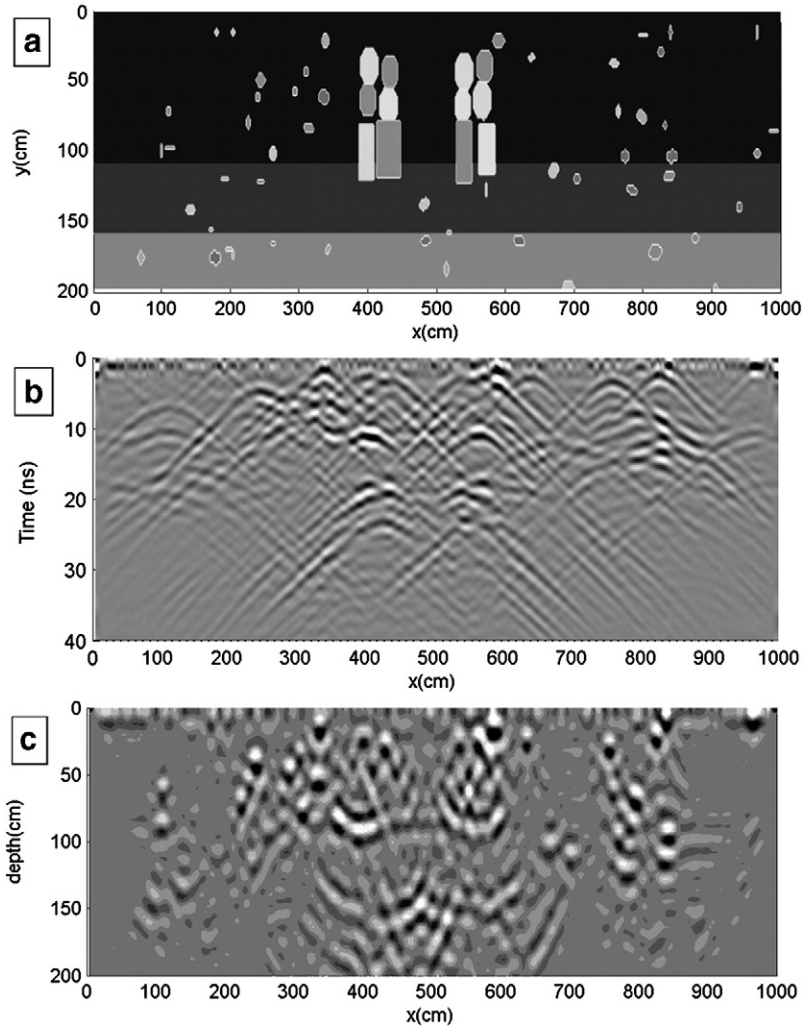

Fig. 7. a) A model for the tomb T3. b) Synthetic radargram for the model shown in a). c) Reverse time migrated section of the data in b).

shallowest diffraction signals in the neighbouring sector NH3, since these signals resulted better-defined and completed than those we obtained in Sector 1, due to the soil and wall conditions. This simple manner of estimating the velocities usually results adequate for such shallow depths, provided that the asymptotic behaviors were achieved. As a check, we compared a number of velocities that could be acceptably obtained from Sector 1 and the velocities that we obtained from NH3: they did not differ (though this result did not assure us that the soil conditions were the same in both prospectings). Unfortunately, we could not detect the base of the walls from the data.

Fig. 5a shows a map of the anomalies that we have related to the buried walls of NH1. A possible layout of walls was also delineated with dashed curves. The resulting diagram shows a complex building, consisting in several walls that seem to delimit at least seven areas. It can be observed that the detected structure, Fig. 5a, agrees with what we interpreted from Sempé's reports, Fig. 5b, in the zone defined by the labels A1 to A6 in Fig. 5a, and labels B1 to B6 in Fig. 5b, both in their forms and dimensions. Moreover, the GPR prospecting reveals the existence of non-reported walls in the western half of NH1. On the other hand, some of the internal walls reported by Sempé in this zone (walls B7–B8, B9–B10, and B10–B11 in Fig. 5b) were not detected by the GPR prospecting; this probably occurred due to a higher deterioration of these narrower walls, mainly during the periods in which they were exposed.

In Fig. 6a we show a photograph of Sector 1, before the excavations tasks, whereas in Fig. 6b we show one of the exposed walls of NH1. Partial excavations, as that in Fig. 6b, were performed in different areas of NH1 in order to confirm the GPR predictions. In all these cases the lateral locations and depths to the tops of the walls were confirmed. Also the hypothesis of collapses and mudflows, which in some cases produced wider effective walls, could be checked.

4. Prospecting of Sector 2

Sector 2 extended along the west and south limits of a former vineyard (Fig. 1b), covering a total area 2700 m^2. The previously excavated tombs, T1 and T2, were approximately located in the central portion of the west side of the farm. For practical reasons we divided Sector 2 into five smaller rectangular sub-sectors, as shown in Fig. 1b. Considering the possibility that linear structures such as fences or walls could also remain buried in the sector, we decided to prospect the area in both orthogonal directions. We defined 1 m×1 m grids in all the sub-sectors.

Contrary to what happened in Sector 1, in Sector 2 we did not have experimental patterns for the signals of the buried targets. Then, as an alternative, we numerically simulated them. To generate synthetic radargrams, a computer program originally developed by Carcione (1996) was extended to include fixed offset configurations.

In Fig. 7a, we show a model for T3: the model consists in a cist built out of rocks. We modeled it without a roof because it was known that all of the tombs had been opened. The forms and dimensions of the tomb were similar to the previously excavated. We assumed relative permittivities for the rocks in the range 7 to 9 and resistivities between 5 and 15 kΩ m; these values included a large number of possible minerals. Two strata were placed at depths 100 cm and 150 cm, respectively. Since the first simulations were performed before the prospecting, the permittivities and resistivities of the strata were estimated from the results obtained in NH3 sector. These values were 3.1, 3.8 and 4.6, for the permittivities, and 10 kΩ m for the resistivity. We also included a number of dispersed rocks, with similar dimensions than those we observed on the surface. Their density was roughly estimated, whereas their locations were established at random. We included maximum fluctuations of 15% for the parameters of the surrounding media, in order to simulate a soil disrupted by agriculture.

The synthetic radargram that resulted from the model in Fig. 7a is shown in Fig. 7b. The electromagnetic response of the walls can be observed between $x=3.8$ m and $x=5.8$ m, and up to 12 ns, approximately. This response is composed of a number of slightly more intense signals than the background, which are distributed in a very irregular form. Two signals that correspond to multiples originated at the upper rocks in the walls can also be seen centered

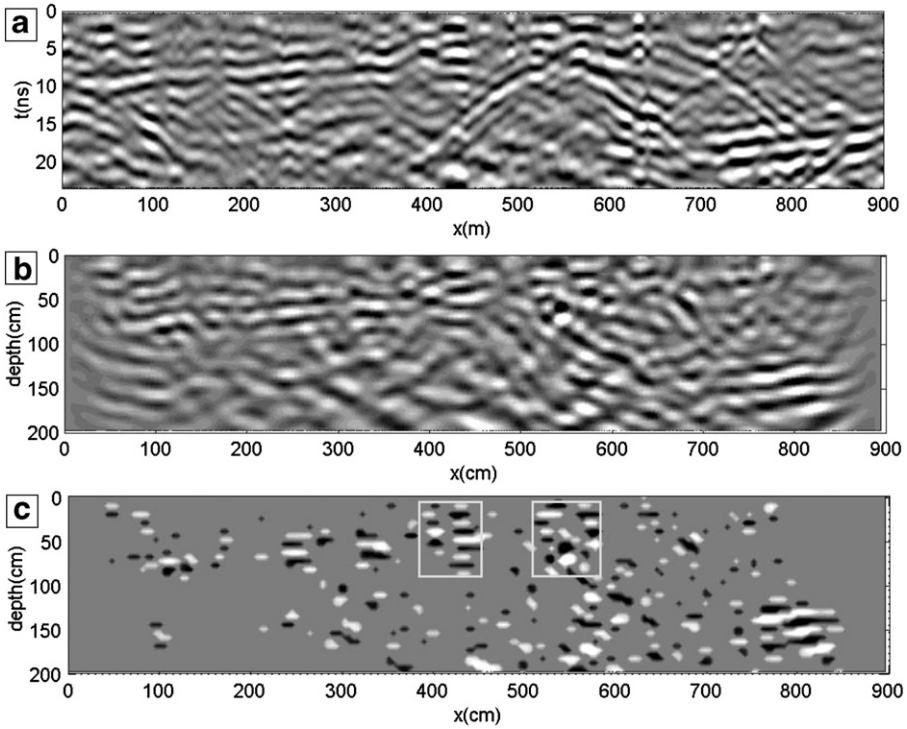

Fig. 8. a) Radargram that corresponds to the $y=8.5$ m profile, in Sector 2. b) Migrated section of the data in figure b). c) The data in b), with a cutoff applied for the highest amplitudes. The selected anomalies are delimited by squares.

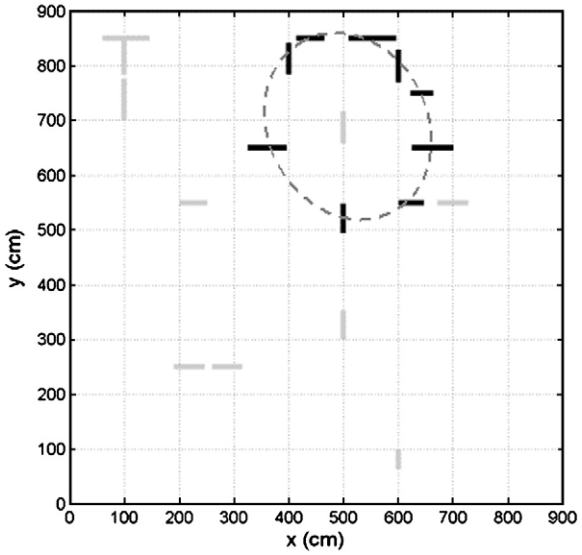

Fig. 9. Map of the GPR anomalies for T3 and their respective interpretation (dashed curve).

at x=4.3 m and x=5.5 m, both at $t \approx 20$ ns, presenting a similar aspect to the wall signals. It can also be observed that the fluctuations in the soil parameters moderately deteriorate the coherence of the main events and that the dispersed rocks produce signals which in many cases overlap and hide those of the walls. Furthermore, groups of these rocks occasionally produce responses very similar to those we searched for (see, for example, the signals around (x, t)=(3.4 m, 5 ns) and (x, t)=(8.3 m, 12 ns).

All these characteristics led us to preview that the direct identification of the signals from the walls in the radargrams acquired in Sector 2 would be very difficult. Then, as a possible way to achieve clearer anomalies, we evaluated the migration of the data. This kind of process presented a number of advantages in relation to the Sector 2 case. Firstly, the migrated profiles often constitute more realistic images of the subsoil, then simplifying the interpretation of the complex structure. Secondly, the focusing process that is implicit in migration was expected to collapse the diffraction hyperbolae and to produce more contrasting and resoluble anomalies for the walls. Finally, the migration of the data also would help in attenuating the multiples, since these kinds of events present different apparent mean velocities than the primary signals.

Fig. 7c shows a reverse time migrated section of the synthetic data in Fig. 7b. We used the mean velocity of the shallower layers for the migration velocity (vm=16.2 cm/ns). As a consequence, the deepest signals appeared a little over-migrated. Despite this, it can be observed that the migration process really produced the desired effects, and that more detectable anomalous regions resulted.

Therefore, the previously described processes were applied to the data acquired in Sector 2. In Fig. 8a we show a characteristic radargram obtained in this sector. As in the case of synthetic data, some regions of the radargram presented signals with slightly higher intensities, but they could not be reasonably defined and identified as possible anomalies due to the walls. This kind of region can be roughly delimited in Fig. 8a in the x-ranges 0–100 cm, 400–450 cm, 530–600 cm, and 720–780 cm, and up to 10 ns.

To estimate the migration velocity (17.0+/−1.4 cm/ns) we proceed as follows. First, we adjusted a hyperbola to each diffraction signal in Sector 2, thus obtaining values for the two way travel time (t0) and the mean velocity of propagation (vp) in the zone above each diffractor. Then, we gathered all the pairs (t0, vp) and from the distribution of these data we finally estimated a range of velocities that were compatible with the expected depths (travel times). The stability of the results was checked in the selected range of velocities, for a representative group of profiles. Then, we used the same mean velocity to migrate all the profiles in Sector 2.

Fig. 8b shows the reverse time migrated section of the data in Fig. 8a. It can be seen in this figure that a moderate improvement in the definition of the anomalies has been obtained through the migration process. Nevertheless, two of the above mentioned zones could be more firmly established as anomalous: these regions extend along the ranges x=400–450 cm and x=530–600 cm, from depths 15 cm to 80 cm, approximately, which resulted compatible with the archeological information about the tombs. On the contrary, the region 720–780 cm was disregarded as an anomalous zone due to its minor relative intensity.

To obtain better visualizations of the possible anomalies in Sector 2, we used an upper cut off for the migrated amplitudes, i.e. we zeroed the (migrated) data whose absolute value was below a predefined threshold. For example, in Fig. 8c we show the image that resulted from Fig. 8b, after the cutoff application. The anomalous zones that we mentioned in the previous paragraph can now be clearly identified in this figure. Other zones extending below 150 cm, smaller than 50 cm in height or narrower than 30 cm were disregarded as anomalies, since they largely contradict the archaeological information.

A group of anomalous regions with similar characteristics to those described in the previous example was detected throughout Sector 2.

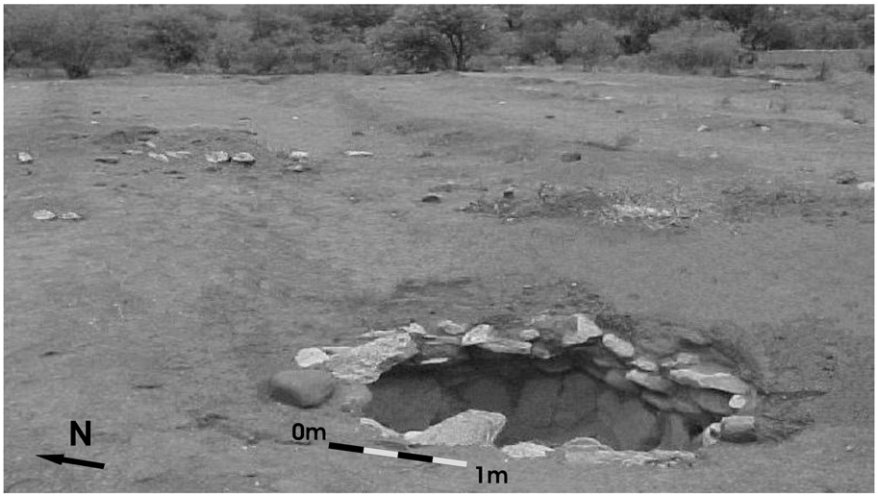

Fig. 10. The tomb T3 after its excavation.

They extended in the vertical direction from approximately 15–30 cm to 75–100 cm, with widths 45–85 cm. They were mapped and interpreted considering the characteristics expected for T3. Fig. 9 is the map of the anomalies in the sub-sector in which we predicted T3. A dotted curve indicates our interpretation.

In Fig. 10 we show T3 after its excavation. The mean diameter of the exposed tomb was measured; a range 2.8–3.2 m was obtained. The walls of T3 extended in depth from 0.15–0.30 m to 1.1–1.2 m, and their widths were 0.5–0.8 m. From these results it can be noted that the lowest depth of the walls resulted greater than that we had estimated (75–100 cm). This fact indicates that the reflections at the interface between the rocks of the base and the soil below were not identified due to their low intensities with respect to other signals. On the contrary, a good agreement between the predicted and the measured data was obtained in relation to all the other parameters.

Although two walls should have been detected in all the GPR profiles that crossed the tomb, only one was detected in some of them (see Fig. 9). In these cases, the failure in the detection probably originated in the combined action of the following factors: the geometry and disposal of the rocks in the walls locally produce lower (anisotropic) effective reflectivities, the permittivity contrasts at the interfaces between the undetected walls and the soil were not high enough, and the disruption of the soil due to agriculture altered the coherence of the events in a manner that this produced a less efficient focusing process when migrating. Despite these problems, which impeded a more precise contouring of T3, the conjunction of forward modeling and migration techniques allowed a precise location of the building. Then we can conclude that the applied methodology has resulted effective in relation to the main objective of this work.

5. Conclusions

In this work we carried out a fast monostatic GPR prospecting of two sectors in Palo Blanco archaeological site, which we called Sector 1 and Sector 2. The objective of this prospecting was to re-localize a missed adobe structure and a cist constructed with rocks. The survey was designed in order to prospect relatively large areas in minimal times. The data was acquired, processed and interpreted. As a consequence, the locations of the residential unit NH1 and the tomb T3 could be satisfactory established and confirmed.

The main adobe walls of the dwelling NH1 were detected in Sector 1. The electromagnetic anomalies due to reflection at the walls were simply identified by comparing the signals in the radargrams with experimental patterns obtained in the neighboring unit NH3. The detected structure resulted more extended than we expected from the previous reports: a number of new walls appeared as a western continuation of NH1.

To analyze the data we acquired in Sector 2, we generated synthetic patterns of the tomb T3. However, these patterns consisted in weak signals that were very difficult to distinguish from other secondary signals. Then, we evaluated the migration of the data. The reverse time process that we applied to the synthetic data resulted in more defined and resolved images of the walls.

Following this methodology, we processed the real data. We confirmed that it was extremely difficult to identify anomalies possibly originated in the walls of T3 directly from the radargrams. Only a number of more intensive zones could be imprecisely delimited at this stage of the analysis. In the next step we migrated the data. As a consequence, many of these zones could be more firmly established or disregarded as anomalies. Then we applied an upper cut off to the migrated amplitude to further improve the visualization of the anomalies. This process finally allowed us to determine a group of anomalies possibly due to the tomb. We drew a map of these anomalies and we interpreted them considering the archaeological information. Therefore, we determine a probable location for T3. The position of this structure was confirmed through an excavation.

As a final comment, we note that the buildings that we have investigated in this work are typical examples of the structures usually found in the NW region of Argentina. The results of this work showed that applying a fast monostatic GPR methodology is an effective strategy to locate these kinds of structures. Then, it is expected that the patterns and methodology we have described in this article will be useful for detecting similar structures in many of the archaeological sites of the region.

Acknowledgements

This work was partially supported by grants from CONICET and ANPCyT.

References

Basile, V., Carrozzo, M., Negri, S., Nuzzo, L., Quarta, T., Villani, A., 2000. A ground-penetrating radar survey for archaeological investigations in an urban area Lecce, Italy. Journal of Applied Geophysics 44, 15–32.

Berard, B., Maillol, J., 2007. Multi-offset ground penetrating radar data for improved imaging in areas of lateral complexity — application at a Native American site. Journal of Applied Geophysics 62, 167–177.

Carcione, J., 1996. Ground radar simulation for archaeological applications. Geophysical Prospecting 44, 871–888.

Conyers, L.B., Goodman, D., 1997. Ground-Penetrating Radar: an Introduction for Archaeologists. Altamira Press, California.

Da Silva Cezar, G., Ferrucio da Rocha, P., Buarque, A., da Costa, A., 2001. Two Brazilian archaeological sites investigated by GPR: Serrano and Morro Grande. Journal of Applied Geophysics 47, 227–240.

De la Vega, M., Osella, A., Lascano, E., Carcione, J., 2005. Ground penetrating radar and geoelectrical simulations of data from the Floridablanca archaeological site. Archaeological Prospection 12, 19–30.

Fisher, E., McMechan, G., Annan, P., Cosway, S., 1992. Examples of reverse-time migration of single-channel, ground-penetrating radar profiles. Geophysics S7, 577–586.

Jaya, M., Botelho, M., Hubral, P., Liebhardt, G., 1999. Remigration of ground-penetrating radar data. Journal of Applied Geophysics 41, 19–30.

Lascano, E., Osella, A., de la Vega, Buscaglia, S., Senatore, X., Lanata, J., 2003. Geophysical prospection at Floridablanca archaeological site, San Julián Bay, Argentina. Archaeological Prospection 10, 175–192.

Leopold, M., Völkel, J., 2004. Neolithic flint mines in Arnhofen, Southern Germany: a ground penetrating radar survey. Archaeological Prospection 11, 57–64.

Linford, N., 2006. The application of geophysical methods to archaeological prospection. Reports on Progress in Physics 69, 2205–2257.

Martino, L., Bonomo, N., Lascano, E., Osella, A., Ratto, N., 2006. Electrical and GPR prospecting at Palo Blanco archaelogical site, northwestern Argentina. Geophysics 71, 193–199.

McClymont, A., Green, A., Streich, R., Horstmeyer, H., Tronicke, J., Nobes, D., Pettinga, J., Campbell, J., Langridge, R., 2008. Visualization of active faults using geometric attributes of 3D GPR data: an example from the Alpine Fault Zone, New Zealand. Geophysics 73, B11–B23.

Nuzzo, L., Leucci, G., Negri, S., Carrozzo, M.T., Quarta, T., 2002. Application of 3D visualization techniques in the analysis of GPR data for archaeology. Annals of Geophysics 45, 321–337.

Osella, A., de la Vega, M., Lascano, E., 2005. 3D electrical imaging of an archaeological site using electric and electromagnetic methods. Geophysics 70, 101–107.

Ratto, N., 2005. La Arqueología del Bolsón de Fiambalá a través de los Estudios de Impacto (Dpto. Tinogasta, Catamarca, Argentina). Actas dos I Jornadas Internacionais Vestígios do Passado. AGIR - Associação para a Investigação e Desenvolvimento Sócio-cultural.

Ratto, N., Martino, L., Feely, A., Osella, A., 2005. Aplicación de Métodos Geofísico al Diseño de Excavación: El Caso del NH-3 de Palo Blanco (Dpto. Tinogasta, Catamarca, Argentina). Primer Congreso Argentino de Arqueometría. Cuaderno de Resúmenes, p. 92.

Ratto, N., Feely, A., Basile, M., 2007. Coexistencia de diseños tecno-estilísticos en el Período Tardío preincaico: el caso del entierro en urna del bebé de La Troya (Tinogasta, Catamarca, Argentina). Revista Intersecciones en Antropología 8, 69–86.

Sempé, M., 1976. Contribution to the archaeology of the Abaucán Valley. PhD thesis, University of La Plata, Buenos Aires, Argentina.

Sempé, M., 1977. Las culturas agroalfareras prehispánicas del valle de Abaucán (Tinogasta-Catamarca). Relaciones de la Sociedad Argentina de Antropología (NS) 11, 55–68.

Sigurdsson, T., Overgaard, T., 1998. Application of GPR for 3D visualization of geological and structural variation in a limestone formation. Journal of Applied Geophysics 40, 29–36.

Symes, W., 2007. Reverse time migration with optimal checkpointing. Geophysics 72, SM213–SM221.

Yilmaz, O., 1987. Seismic data processing. Society of Exploration Geophysicists, Tulsa, OK.